

Power-efficient and Secure WPCNs with Residual Hardware Impairments and a Non-linear EH Model

Elena Boshkovska*, Derrick Wing Kwan Ng[†], and Robert Schober*

*Friedrich-Alexander-University Erlangen-Nürnberg (FAU), Germany

[†]The University of New South Wales, Australia

Abstract—In this paper, we design a resource allocation algorithm for a wireless-powered communication network (WPCN) taking into account residual hardware impairments (HWIs) at the transceivers and the non-linearity of radio frequency (RF) energy harvesting (EH) circuits. In order to ensure communication secrecy, physical layer (PHY) security techniques are exploited to deliberately degrade the channel quality of a multiple-antenna eavesdropper. The resource allocation algorithm design is formulated as a non-convex optimization problem for the minimization of the total consumed power in the network, while guaranteeing the quality of service (QoS) of the information receivers (IRs). The globally optimal solution of the optimization problem is obtained via a one-dimensional search and semidefinite programming (SDP) relaxation. Numerical results demonstrate that the proposed scheme can significantly reduce the power consumption of the system compared to a baseline scheme, which assumes ideal hardware.

I. INTRODUCTION

Wireless charging of battery-powered wireless devices in wireless communication networks via wireless power transfer (WPT) technology could prolong the lifetime of the networks. In fact, the concept of wireless-powered communication networks (WPCNs), where wireless devices are powered via radio frequency (RF) electromagnetic waves, has gained a lot of attention recently in the context of enabling sustainability via WPT [1]. In particular, it is expected that the number of interconnected wireless devices could increase to up to 50 billion by 2020 [2]. A large portion of these wireless devices, some of which may be inaccessible for frequent battery replacement, could be powered by dedicated power stations via RF-based WPT to facilitate their information transmissions [3]. It is noted that RF-based WPT offers a more stable and controllable source of energy compared to other natural energy sources, such as solar, wind, etc., which are usually climate and location dependent. On the other hand, the large number of wireless devices encourages the use of low-quality and low-cost hardware components in order to reduce the deployment costs of wireless networks. Yet, RF transceivers with cheap hardware components suffer from various kinds of hardware impairments (HWIs). These HWIs are caused by non-linear power amplifiers, frequency and phase offsets, in-phase and quadrature (I/Q) imbalance, and quantization noise [4]. Although the negative impact on the system performance caused by these HWIs can be reduced by calibration and compensation algorithms, residual distortions that depend on the power of the desired signal are still present at the transceivers [4], [5]. Hence, existing resource allocation algorithms for multi-user wireless networks [3], [6]–[8] designed based on the assumption of ideal hardware may lead to performance losses in practical systems.

The increasing number of wireless devices also poses a threat to communication security in future wireless networks due to the enormous amounts of data transmitted over wireless channels [3], [9]. Nowadays, wireless communication security is achieved with cryptographic encryption algorithms at the application layer. Unfortunately, these traditional security methods may not be applicable to future wireless networks with large numbers of users, since encryption algorithms usually require secure secret key distribution and management via an authenticated third party. Recently, physical layer (PHY) security has been proposed as an effective complementary technology to the existing encryption algorithms for providing secure communication [3], [6]–[11]. Specifically, PHY security exploits the unique characteristics of wireless channels, such as fading, noise, and interference [9], to protect the communication between legitimate devices from eavesdropping. In this context, the authors of [3] designed a resource allocation algorithm that jointly optimizes the transmit power, transfer time, and spatial beam to facilitate security in WPCNs. However, most of the existing works on secure WPT systems were based on the assumption of ideal hardware [3], [7]–[8]. In contrast, the work in [10] considered the analysis and design of secure massive multiple-input multiple-output (MIMO) systems in the presence of a passive eavesdropper and different HWIs at the transceivers. Besides, the authors of [12] studied the impact of residual HWIs on the performance of a WPT system. Specifically, [12] considered residual HWIs in a two-way WPT-based cognitive relay network, where the relay is powered by harvesting energy from the signals transmitted by the source. The numerical results in [12] demonstrated that an increase in the residual HWIs significantly deteriorates the outage probability and the throughput performance of the considered WPT-based relay network. Hence, the results from [3], [7]–[8] related to secure WPT systems may not be valid for practical implementations where HWIs exist. On the other hand, the work in [12] neglected the security aspects in the considered WPT system. Besides, [12] assumed an overly simplified linear energy harvesting (EH) model for the end-to-end WPT characteristic. Yet, measurements on practical EH circuits demonstrated a highly non-linear end-to-end WPT characteristic [13], which implies that transmission schemes and algorithms designed based on the conventional linear EH model may cause performance degradation in practical implementations. Moreover, [12] also neglected the circuit power consumption and the inefficiency of power amplifiers, which are present in practical wireless devices.

To address the above issues, we propose a power-efficient resource allocation algorithm design for providing communication secrecy in WPCNs, where residual HWIs at the transceivers and a practical non-linear EH model are taken into account. The resource allocation algorithm design is formulated as a non-convex optimization problem for the minimization of the

R. Schober is supported by the AvH Professorship Program of the Alexander von Humboldt Foundation. D. W. K. Ng is supported under Australian Research Council's Discovery Early Career Researcher Award funding scheme (project number DE170100137).

total consumed power, while guaranteeing the quality of service (QoS) at the information receivers (IRs). The optimal solution of the proposed problem is obtained via a one-dimensional search and semidefinite programming (SDP) relaxation. The solution of the resulting equivalent optimization problem unveils that information beamforming from the AP in the direction of the IRs is optimal and that the SDP relaxation is tight. Numerical results demonstrate that the proposed scheme can significantly reduce the power consumption in the considered WPCN compared to a baseline scheme designed under the assumption of ideal hardware.

II. SYSTEM MODEL

In this section, we first present the considered system model, and then discuss the energy harvesting and hardware impairment models assumed for resource allocation algorithm design.

A. Notation

We use boldface capital and lower case letters to denote matrices and vectors, respectively. \mathbf{A}^H , $\text{Tr}(\mathbf{A})$, $\det(\mathbf{A})$, \mathbf{A}^{-1} , and $\text{Rank}(\mathbf{A})$ represent the Hermitian transpose, trace, determinant, inverse, and rank of matrix \mathbf{A} , respectively; $\mathbf{A} \succeq \mathbf{0}$ indicates that \mathbf{A} is a positive semidefinite matrix; matrix \mathbf{I}_N denotes the $N \times N$ identity matrix. $\mathbb{C}^{N \times M}$ denotes the space of all $N \times M$ matrices with complex entries. \mathbb{H}^N represents the set of all N -by- N complex Hermitian matrices. $|\cdot|$ and $\|\cdot\|_F$ represent the absolute value of a complex scalar and the Frobenius norm, respectively. The distribution of a circularly symmetric complex Gaussian (CSCG) vector with mean vector \mathbf{x} and covariance matrix Σ is denoted by $\mathcal{CN}(\mathbf{x}, \Sigma)$, and \sim means “distributed as”. $\mathcal{E}\{\cdot\}$ denotes statistical expectation. $[x]^+$ stands for $\max\{0, x\}$. $\nabla_{\mathbf{x}} f(\mathbf{x})$ represents the partial derivative of function $f(\mathbf{x})$ with respect to the elements of vector \mathbf{x} . Furthermore, $\text{diag}[\mathbf{x}]$ is a diagonal matrix with the elements of \mathbf{x} on the main diagonal. $[\mathbf{A}]_{n,n}$ returns the element in the n -th row and n -th column of square matrix \mathbf{A} .

B. System Model

We focus on a WPCN, comprising a power station¹ (PS), an access point (AP), K IRs, and one eavesdropper (Eve), cf. Figure 1. We assume that the PS, the AP, and Eve are equipped with $N_{\text{PS}} \geq 1$, $N_{\text{AP}} \geq 1$, and $N_{\text{EV}} \geq 1$ antennas, respectively. The IRs are single-antenna devices with simple hardware. We note that an eavesdropper equipped with N_{EV} antennas is equivalent to multiple eavesdroppers with a total of N_{EV} antennas which are connected to a joint processing unit.

The communication in the system comprises two transmission phases as shown in Figure 1. We assume that the fading channels in both phases are frequency flat and slowly time-varying, and that the channel state information (CSI) is available for resource allocation. Phase I with a duration of τ_I is reserved for wireless charging (WC), where the PS transmits a dedicated energy beam to the energy-constrained AP. The instantaneous received signal at the AP during Phase I is given by

$$\mathbf{y}_{\text{AP}} = \mathbf{L}^H(\mathbf{v} + \boldsymbol{\xi}^{(t)}) + \boldsymbol{\xi}^{(r)} + \mathbf{n}_{\text{AP}}, \quad (1)$$

where $\mathbf{v} \in \mathbb{C}^{N_{\text{PS}} \times 1}$ is the energy signal vector adopted in Phase I for WC with covariance matrix $\mathbf{V} = \mathcal{E}\{\mathbf{v}\mathbf{v}^H\}$. The channel matrix between the PS and the AP is denoted by $\mathbf{L} \in \mathbb{C}^{N_{\text{PS}} \times N_{\text{AP}}}$ and captures the joint effect of path loss and multipath fading.

¹In this work, we assume that the PS is connected to the main grid with a continuous and stable energy supply.

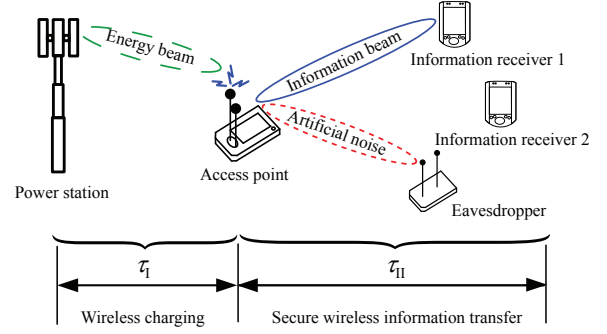


Fig. 1. A WPCN employing two transmission phases.

Vector $\mathbf{n}_{\text{AP}} \sim \mathcal{CN}(\mathbf{0}, \sigma_n^2 \mathbf{I}_{N_{\text{AP}}})$ represents the additive white Gaussian noise (AWGN) at the AP where σ_n^2 denotes the noise variance at each antenna of the AP. In (1), $\boldsymbol{\xi}^{(t)} \in \mathbb{C}^{N_{\text{PS}} \times 1}$ and $\boldsymbol{\xi}^{(r)} \in \mathbb{C}^{N_{\text{AP}} \times 1}$ represent the residual HWIs after compensation at the transmitter and receiver side during Phase I, respectively. The model adopted for the residual HWIs will be presented in the next section.

In Phase II, which has a duration of τ_{II} , the AP transmits K independent signals to K IRs simultaneously. Due to the broadcast nature of the wireless channel, there is a potential eavesdropping threat. In order to circumvent this threat, the AP deliberately emits artificial noise (AN) to degrade the channel quality of the eavesdropper [9]. Moreover, we assume that the PS is silent during Phase II. The instantaneous received signal at IR k in Phase II is given by

$$y_{\text{IR}_k} = \mathbf{h}_k^H \left(\sum_{k=1}^K \mathbf{w}_k s_k + \mathbf{u} + \boldsymbol{\zeta}^{(t)} \right) + \varsigma_k^{(r)} + n_{\text{IR}_k}, \quad (2)$$

where $s_k \in \mathbb{C}$ and $\mathbf{w}_k \in \mathbb{C}^{N_{\text{AP}} \times 1}$ are the information symbol and the corresponding beamforming vector, respectively. Without loss of generality, we assume that $\mathcal{E}\{|s_k|^2\} = 1, \forall k$. $\mathbf{h}_k \in \mathbb{C}^{N_{\text{AP}} \times 1}$ is the channel vector between the AP and IR k . $\mathbf{u} \in \mathbb{C}^{N_{\text{AP}} \times 1}$ is the AN vector, with covariance matrix $\mathbf{U} = \mathcal{E}\{\mathbf{u}\mathbf{u}^H\}$, exploited by the AP to degrade the channel quality of the eavesdropper. $\boldsymbol{\zeta}^{(t)} \in \mathbb{C}^{N_{\text{AP}} \times 1}$ is the distortion vector due to the residual transmit HWIs at the AP, while $\varsigma_k^{(r)} \in \mathbb{C}$ represents the residual receiver HWIs at IR k . $n_{\text{IR}_k} \sim \mathcal{CN}(0, \sigma_{\text{IR}_k}^2)$ is the AWGN at IR k , with noise power $\sigma_{\text{IR}_k}^2$. The instantaneous received signal at the eavesdropper in Phase II is given by

$$\mathbf{y}_{\text{E}} = \mathbf{G}^H \left(\sum_{k=1}^K \mathbf{w}_k s_k + \mathbf{u} + \boldsymbol{\zeta}^{(t)} \right) + \mathbf{n}_{\text{E}}, \quad (3)$$

where $\mathbf{G} \in \mathbb{C}^{N_{\text{AP}} \times N_{\text{E}}}$ denotes the channel matrix between the AP and Eve. $\mathbf{n}_{\text{E}} \sim \mathcal{CN}(\mathbf{0}, \sigma_{\text{E}}^2 \mathbf{I}_{N_{\text{E}}})$ is the AWGN vector at the eavesdropper, with noise power σ_{E}^2 . In this work, we assume that ideal hardware is available at the eavesdropper which constitutes the worst case for communication security. Additionally, although it may not be possible to obtain the CSI or the location of eavesdroppers in many practical applications, we assume that Eve’s CSI is available for resource allocation, in order to concentrate on the impact of HWIs on the system performance, which is the main focus of this paper².

²For resource allocation algorithm design, the effect of imperfect CSI can be modeled based on deterministic or probabilistic uncertainty models, see e.g. [3], [6], [14]. Imperfect CSI and its impact on the performance of the considered system will be taken into account in a future extension of this work.

C. Hardware Impairment Model

In this paper, we adopt the general HWI model proposed in [15, Chapter 7]. In particular, the residual distortion caused by the aggregate effect of different HWIs, such as I/Q imbalance, phase noise, and power amplifier non-linearities is modeled as a Gaussian random variable whose variance scales with the power of the useful signal at the transceiver. This model has been widely used in the literature to study the effects of transceiver HWIs on the performance of various communication systems [4], [5], [12]. Besides, the authors of [5] showed that this model accurately captures the residual distortions caused by the joint effect of various HWIs for practical multiple-antenna systems.

Hence, the distortion noise caused by the transmitter HWIs at the PS in (1) is modeled as $\xi^{(t)} \sim \mathcal{CN}(\mathbf{0}, \Phi)$, where $\Phi \in \mathbb{C}^{N_{\text{PS}} \times N_{\text{PS}}}$ is a diagonal covariance matrix, which contains the distortion noise variances at each antenna of the PS on its main diagonal, and is given by

$$\Phi = \text{diag} \left[\eta_1^2 \left(\sqrt{P_{\text{av},1}^{\text{PS}}} \right), \dots, \eta_{N_{\text{PS}}}^2 \left(\sqrt{P_{\text{av},N_{\text{PS}}}^{\text{PS}}} \right) \right]. \quad (4)$$

In (4), $P_{\text{av},m}^{\text{PS}} = \mathcal{E}\{\|\mathbf{S}_m \mathbf{v}\|_F^2\} = [\mathbf{V}]_{m,m}$, $m \in \{1, \dots, N_{\text{PS}}\}$, is the average power of the transmit signal at the m -th antenna of the PS, where \mathbf{S}_m is a matrix with all entries equal to 0 except for the m -th diagonal element which is equal to 1. $\eta_m(\cdot)$, $\forall m$, is a convex, continuous, and monotonically increasing distortion function which maps the square root of the average power of the transmit signal to a specific distortion value. A commonly adopted example for modeling the transmitter distortion function is given by [4]

$$\eta_m(x_m) = \frac{k_1}{100} x_m \left(1 + \left(\frac{x_m}{k_2} \right)^4 \right) [\sqrt{\text{mW}}], \quad (5)$$

where x_m is the square root of the average transmit power at antenna m . Constants k_1 and k_2 are model parameters which should be chosen such that they fit the measurements of the error vector magnitude (EVM) of practical systems. Similarly, the transmitter HWIs at the AP in Phase II are modeled as $\zeta^{(t)} \sim \mathcal{CN}(\mathbf{0}, \Psi)$ with covariance matrix

$$\Psi = \text{diag} \left[\eta_1^2 \left(\sqrt{P_{\text{av},1}^{\text{AP}}} \right), \dots, \eta_{N_{\text{AP}}}^2 \left(\sqrt{P_{\text{av},N_{\text{AP}}}^{\text{AP}}} \right) \right], \quad (6)$$

where $P_{\text{av},n}^{\text{AP}} = \mathcal{E}\{\|\mathbf{S}_n(\sum_{k=1}^K \mathbf{w}_k s_k + \mathbf{u})\|_F^2\} = [\sum_{k=1}^K \mathbf{w}_k \mathbf{w}_k^H + \mathbf{U}]_{n,n}$, $\forall n \in \{1, \dots, N_{\text{AP}}\}$. On the other hand, the received signal is affected mostly by phase noise and I/Q imbalances [15, Chapter 7]. In the considered WPCN, these residual HWIs are modeled by the receiver distortion noise at the AP, $\xi^{(r)} \in \mathbb{C}^{N_{\text{AP}} \times 1}$, cf. (1), where $\xi^{(r)} \sim \mathcal{CN}(\mathbf{0}, \sigma_{\text{dAP}}^2 \mathbf{I}_{N_{\text{AP}}})$. Moreover, $\sigma_{\text{dAP}} = \nu(\sqrt{\mathcal{E}\{\|\mathbf{L}^H \mathbf{v}\|_F^2\}})$ and $\nu(\cdot)$ is a convex, continuous, and monotonically increasing function that models the receiver impairment characteristic. Additionally, the receiver HWIs at each IR during Phase II are given by $\zeta_k^{(r)} \sim \mathcal{CN}(0, \sigma_{\text{dIR}_k}^2)$, with $\sigma_{\text{dIR}_k} = \nu(\sqrt{\mathcal{E}\{\|\mathbf{h}_k^H(\sum_{k=1}^K \mathbf{w}_k s_k + \mathbf{u})\|_F^2\}})$. According to [4], the receiver distortion function can be modeled as $\nu(x) = \frac{k_3}{100} x$, where x is the square root of the power of the received signal and k_3 is a model parameter.

D. Energy Harvesting Model

In the considered WPCN, we exploit the signals transmitted by the PS in Phase I to charge the AP and facilitate secure

information transfer in Phase II. In this paper, we adopt the non-linear EH model from [16] to characterize the end-to-end WPT at the AP. The total energy harvested by the AP in Phase I is given by

$$\Xi_{\text{tot}}(\theta) = \frac{\frac{M}{1+\exp(-a(\theta-b))} - M\Omega}{1-\Omega}, \Omega = \frac{1}{1+\exp(ab)}, \quad (7)$$

$$\theta = \text{Tr}(\mathbf{L}^H (\mathbf{V}_I + \Phi) \mathbf{L}),$$

where θ represents the received RF power at the AP. The parameters M , a , and b in (7) capture the joint effects of various non-linear phenomena caused by hardware limitations in practical EH circuits. More specifically, M represents the maximum power that can be harvested by the EH circuit, as the circuit gets saturated for large received RF powers. Moreover, a and b are related to different physical hardware phenomena, such as circuit sensitivity limitations and current leakage. In fact, the non-linear EH model was shown to accurately characterize the behaviour of various practical EH circuits [14], [16]. In contrast, the conventional linear EH model, which is widely used in the literature [3], [7]–[8], [12], may lead to severe model mismatches in resource allocation algorithm design, and as a result, cause performance degradation.

III. RESOURCE ALLOCATION PROBLEM FORMULATION

In this section, we first define the system performance metrics adopted for algorithm design, and then we formulate the resource allocation optimization problem.

A. Achievable Data Rate and Secrecy Rate

The achievable data rate of IR k in Phase II is given by

$$R_k = \tau_{\text{II}} \log_2 (1 + \Gamma_k), \quad \text{where} \quad (8)$$

$$\Gamma_k = \frac{\text{Tr}(\mathbf{W}_k \mathbf{H}_k)}{\sum_{j \neq k} \text{Tr}(\mathbf{W}_j \mathbf{H}_k) + \text{Tr}(\mathbf{U} \mathbf{H}_k) + \text{Tr}(\Psi \mathbf{H}_k) + \sigma_{\text{dIR}_k}^2 + \sigma_n^2}$$

is the receive signal-to-interference-plus-noise ratio (SINR) at IR k , and we employ $\mathbf{W}_k = \mathbf{w}_k \mathbf{w}_k^H$ and $\mathbf{H}_k = \mathbf{h}_k \mathbf{h}_k^H$, $\forall k$.

Since the AP does not know the computational capabilities of the eavesdropper, we assume the worst-case scenario for facilitating secrecy provisioning. In the considered worst case, the eavesdropper is able to remove all multiuser interference via successive interference cancellation, and only attempts to decode the information of IR k . As a result, the capacity at the eavesdropper for decoding the information intended for IR k is given by

$$C_k = \tau_{\text{II}} \log_2 \det \left(\mathbf{I}_{N_E} + \mathbf{Q}^{-1} \mathbf{G}^H \mathbf{W}_k \mathbf{G} \right), \quad (9)$$

where $\mathbf{Q} = \mathbf{G}^H (\mathbf{U} + \Psi) \mathbf{G} + \sigma_E^2 \mathbf{I}_{N_E}$ is the interference-plus-noise covariance matrix of the eavesdropper. The achievable secrecy rate between the AP and IR k is given by

$$R_k^{\text{sec}} = [R_k - C_k]^+. \quad (10)$$

B. Total Power Consumption

In this section, we study the power consumption in both transmission phases. Due to the residual HWIs at the transmitter of the PS, a portion of the transmitted power is wasted during Phase I. More specifically, the total power consumption in Phase

I is given by

$$P_{\text{PS-I}} = \rho_{\text{PS}} \left(\underbrace{\text{Tr}(\mathbf{V})}_{\text{power for charging}} + \underbrace{\text{Tr}(\Phi)}_{\text{power waste}} \right) + P_{\text{cps}}, \quad (11)$$

where P_{cps} accounts for the constant circuit power consumption at the PS. Besides, to capture the power inefficiency of power amplifiers, we introduce a linear multiplicative constant $\rho_{\text{PS}} > 1$ for the power radiated by the PS [7]. For example, if $\rho_{\text{PS}} = 5$, then for every 1 Watt of power radiated in the RF, the PS consumes 5 Watt of power which leads to a power amplifier efficiency of 20%. Afterwards, in Phase II, the AP sends K independent information signals to the K IRs concurrently. Besides, AN is emitted by the AP to degrade the channel of the eavesdropper. Because of the residual transmit HWIs at the AP, a portion of the power is also wasted during Phase II. Hence, the total power consumption in Phase II is given by

$$P_{\text{AP-II}} = \rho_{\text{AP}} \left(\underbrace{\sum_{k=1}^K \text{Tr}(\mathbf{W}_k)}_{\text{power for information transmission}} + \underbrace{\text{Tr}(\mathbf{U})}_{\text{power for jamming}} + \underbrace{\text{Tr}(\Psi)}_{\text{power waste}} \right) + P_{\text{cAP}}. \quad (12)$$

Here, P_{cAP} is a positive constant circuit power consumption and $\rho_{\text{AP}} > 1$ denotes the power amplifier inefficiency at the AP.

C. Optimization Problem Formulation

In the following, we formulate the optimization problem for the minimization of the total power consumption in both transmission phases while guaranteeing secure communication in the considered WPCN. The optimization problem is given by:

$$\begin{aligned} & \underset{\tau_1, \tau_{\text{II}}, \theta, \mathbf{V} \in \mathbb{H}^{N_{\text{PS}}}, \mathbf{U} \in \mathbb{H}^{N_{\text{AP}}}, \mathbf{W}_k \in \mathbb{H}^{N_{\text{AP}}}}{\text{minimize}} && \tau_1 P_{\text{PS-I}} + \tau_{\text{II}} P_{\text{AP-II}} \end{aligned} \quad (13)$$

$$\begin{aligned} \text{s.t.} \quad \text{C1:} & \tau_{\text{II}} \log_2(1 + \Gamma_k) \geq R_{\text{req}_k}, \forall k, \\ \text{C2:} & \tau_{\text{II}} \log_2 \det \left(\mathbf{I}_{N_E} + \mathbf{Q}^{-1} \mathbf{G}^H \mathbf{W}_k \mathbf{G} \right) \leq R_{\text{tol}}, \forall k, \\ \text{C3:} & \tau_1 + \tau_{\text{II}} = T_{\text{max}}, \\ \text{C4:} & \tau_{\text{II}} \left(P_{\text{cAP}} + \rho_{\text{AP}} \left(\sum_{k=1}^K \text{Tr}(\mathbf{W}_k) + \text{Tr}(\mathbf{U}) + \text{Tr}(\Psi) \right) \right) \\ & \leq \tau_1 \Xi_{\text{tot}}(\theta) + E_{\text{res}}, \\ \text{C5:} & \theta \leq \text{Tr}(\mathbf{L}^H (\mathbf{V} + \Phi) \mathbf{L}), \\ \text{C6:} & \mathbf{W}_k \succeq \mathbf{0}, \forall k, \mathbf{V}, \mathbf{U} \succeq \mathbf{0}, \text{C7: } \tau_1, \tau_{\text{II}} \geq 0, \\ \text{C8:} & \text{Rank}(\mathbf{W}_k) \leq 1, \forall k. \end{aligned}$$

The objective function in (13) takes into account the total power consumption in Phases I and II at the PS and AP³, cf. (11) and (12), respectively. Constraint C1 ensures a minimum required data rate R_{req_k} for IR k . On the other hand, R_{tol} in C2 limits the maximum tolerable data rate at Eve. In practice, $R_{\text{req}_k} \gg R_{\text{tol}} > 0$ is set by the system operator to ensure secure communication⁴. T_{max} in constraint C3 specifies the total time available for both phases. C4 is a constraint on the

³We optimize the power consumption in both phases, even though the AP is wirelessly charged by the PS only in Phase I, since besides the energy harvested in Phase I, the AP can also use the available residual energy E_{res} for transmission in Phase II, cf. constraint C4. Hence, the power consumption of Phase II should also be minimized.

⁴We note that (13) guarantees a minimum secrecy rate of $R_k^{\text{sec}} = R_{\text{req}_k} - R_{\text{tol}}$ for IR k .

overall energy consumption at the AP during Phase II. The total available energy at the AP comprises the energy harvested from the dedicated energy signal transmitted by the PS in Phase I, and a constant energy $E_{\text{res}} \geq 0$, which may represent the residual energy at the AP from previous transmissions or energy obtained from other sources. Furthermore, θ in C5 is an auxiliary optimization variable which represents the received RF power at the AP. Constraint C6 ensures that \mathbf{W}_k , \mathbf{V} , and \mathbf{U} are positive semidefinite matrices. C7 is a non-negativity constraint on the durations of Phase I and Phase II, respectively. $\mathbf{W}_k \succeq \mathbf{0}$, $\mathbf{W}_k \in \mathbb{H}^{N_{\text{AP}}}$, $\forall k$, and constraint C8 are imposed to guarantee that $\mathbf{W}_k = \mathbf{w}_k \mathbf{w}_k^H$, $\forall k$, holds after optimization.

IV. RESOURCE ALLOCATION ALGORITHM DESIGN

The resource allocation problem in (13) is a non-convex optimization problem because the right-hand side of constraint C4 is a quasiconcave function with respect to τ_1 and θ and the combinatorial nature of constraint C8, which is difficult to handle. Moreover, the optimization variables are coupled in the objective function and constraint C4. Besides, the log-det function in constraint C2 is intractable in its current form.

Furthermore, the covariance matrices of the HWI vectors, Φ and Ψ , affect the optimization variables, \mathbf{V} , \mathbf{U} , and \mathbf{W}_k , and the constraints containing these covariance matrices are non-convex in their current form [4]. Hence, in order to facilitate the design of a computationally efficient resource allocation algorithm, we first introduce auxiliary optimization matrices, $\mathbf{B}_{\text{PS}} \in \mathbb{C}^{N_{\text{PS}} \times N_{\text{PS}}}$ and $\mathbf{B}_{\text{AP}} \in \mathbb{C}^{N_{\text{AP}} \times N_{\text{AP}}}$, which account for the hardware impairments at the PS and the AP, respectively. Additionally, we introduce auxiliary optimization variables, $r_{\text{IR},k}$, $\forall k$, which represent the distortion noise terms caused by the receiver HWIs at the IRs. Then, we transform problem (13) into the following equivalent⁵ rank-constrained SDP optimization problem with respect to the optimization variable set $\mathcal{P} = \{\tau_1, \tau_{\text{II}}, \mathbf{W}_k, \mathbf{V}, \mathbf{U}, \theta, \mathbf{B}_{\text{AP}}, \mathbf{B}_{\text{PS}}, r_{\text{IR},k}\}$:

$$\begin{aligned} & \underset{\mathcal{P}}{\text{minimize}} && \tau_1 \tilde{P}_{\text{PS-I}} + \tau_{\text{II}} \tilde{P}_{\text{AP-II}} \end{aligned} \quad (14)$$

$$\begin{aligned} \text{s.t.} \quad \widetilde{\text{C1:}} & \frac{\text{Tr}(\mathbf{H}_k \mathbf{W}_k)}{\Gamma_{\text{req}_k}} \geq \sum_{j \neq k} \text{Tr}(\mathbf{W}_j \mathbf{H}_k) + \text{Tr}(\mathbf{U} \mathbf{H}_k) \\ & + \sum_{n=1}^{N_{\text{AP}}} \text{Tr}(\mathbf{S}_n \mathbf{B}_{\text{AP}} \mathbf{H}_k) + r_{\text{IR},k}^2 + \sigma_n^2, \forall k, \\ \widetilde{\text{C2:}} & \frac{\mathbf{G}^H \mathbf{W}_k \mathbf{G}}{\Gamma_{\text{tol}}} \preceq \mathbf{G}^H (\mathbf{U} + \mathbf{B}_{\text{AP}}) \mathbf{G} + \sigma_{\text{E}}^2 \mathbf{I}_E, \forall k, \\ \widetilde{\text{C4:}} & \tau_{\text{II}} \tilde{P}_{\text{AP-II}} \leq \tau_1 \Xi_{\text{tot}}(\theta) + E_{\text{res}}, \text{C3, C6, C7,} \\ \widetilde{\text{C5:}} & \theta \leq \text{Tr}(\mathbf{L}^H (\mathbf{V} + \mathbf{B}_{\text{PS}}) \mathbf{L}), \\ \text{C8:} & \text{Rank}(\mathbf{W}_k) \leq 1, \forall k, \text{C9: } \mathbf{B}_{\text{PS}}, \mathbf{B}_{\text{AP}} \succeq \mathbf{0}, \\ \text{C10:} & \eta_n \left(\sqrt{\left[\sum_{k=1}^K \mathbf{W}_k + \mathbf{U} \right]_{n,n}} \right) \leq \sqrt{[\mathbf{B}_{\text{AP}}]_{n,n}}, \forall n, \\ \text{C11:} & \eta_m \left(\sqrt{[\mathbf{V}]_{m,m}} \right) \leq \sqrt{[\mathbf{B}_{\text{PS}}]_{m,m}}, \forall m, \\ \text{C12:} & \nu \left(\sqrt{\text{Tr}(\mathbf{H}_k (\sum_{t=1}^K \mathbf{W}_t + \mathbf{U}))} \right) \leq r_{\text{IR},k}, \forall k, \end{aligned}$$

where $\Gamma_{\text{req}_k} = 2^{R_{\text{req}_k}/\tau_{\text{II}}} - 1$, $\Gamma_{\text{tol}} = 2^{R_{\text{tol}}/\tau_{\text{II}}} - 1$, and the power consumption equations for Phase I and Phase II are

⁵In this paper, equivalent means that the transformed problem and the original problem share the same optimal solution.

TABLE I
SIMULATION PARAMETERS.

Carrier center frequency	915 MHz
Bandwidth	200 kHz
Path loss exponent	2
PS to AP fading distribution	Rician, Rician factor 3 dB
AP to IRs, Eve fading distribution	Rayleigh
PS and AP antenna gain	10 dBi and 8 dBi
Noise power	$\sigma_n^2 = \sigma_{IR}^2 = \sigma_E^2 = -110$ dBm
Power amplifier efficiency	$1/\rho_{PS} = 1/\rho_{AP} = 40\%$
Circuit power consumption	$P_{CPS} = P_{CAP} = 5 \mu\text{W}, \forall k$
Non-linear EH model parameters	$M = 24$ mW, $a=150$, $b = 0.0014$ [13]
Distance PS-to-AP, AP-to-IR, AP-to-Eve	10 m, 50 m, 80 m

rewritten as

$$\tilde{P}_{PS-I} = \rho_{PS} \left(\text{Tr}(\mathbf{V}) + \sum_{m=1}^{N_{PS}} \text{Tr}(\mathbf{S}_m \mathbf{B}_{PS}) \right) + P_{CPS}, \text{ and} \quad (15)$$

$$\tilde{P}_{AP-II} = \rho_{AP} \left(\sum_{k=1}^K \text{Tr}(\mathbf{W}_k) + \text{Tr}(\mathbf{U}) + \sum_{n=1}^{N_{AP}} \text{Tr}(\mathbf{S}_n \mathbf{B}_{AP}) \right) + P_{CAP},$$

respectively. Furthermore, constraint C2 in (13) is replaced by constraint $\tilde{C}2$ in (14). These two constraints are equivalent when $R_{tol} > 0$ and $\text{Rank}(\mathbf{W}_k) \leq 1$ hold, cf. [6, Proposition 1].

Next, we handle the coupling of the optimization variables in the objective function and constraint C4. In particular, we fix τ_I and $\tau_{II} = T_{\max} - \tau_I$, cf. constraint C3, and solve (14) for the remaining optimization variables. By assuming a fixed τ_I the quasiconcavity of the right-hand side of constraint C4 is also resolved. In particular, for a given τ_I , the right-hand side of constraint C4 is concave with respect to θ .

The remaining obstacle for the convexity of (14) is the rank-one constraint C8. Hence, in order to obtain a computationally efficient resource allocation, we adopt SDP relaxation and remove constraint C8.

For given τ_I and τ_{II} , the equivalent SDP relaxed formulation of (14) is given by:

$$\begin{aligned} & \underset{\mathcal{P}}{\text{minimize}} \quad \tau_I \tilde{P}_{PS-I} + \tau_{II} \tilde{P}_{AP-II} \\ & \text{s.t.} \quad \tilde{C}1, \tilde{C}2, \tilde{C}4, \tilde{C}5, C6, C7, C10-C12. \end{aligned} \quad (16)$$

The optimization problem⁶ in (16) is a standard convex optimization problem and can be solved efficiently by numerical convex program solvers such as CVX [17]. However, by solving (16) numerically, there is no guarantee that the optimal solution satisfies C8 of the original problem formulation in (13), i.e., $\text{Rank}(\mathbf{W}_k) \leq 1, \forall k$. Hence, we study the structure of the solution of the SDP relaxed problem in (16) in the following Theorem.

Theorem 1. *Suppose that the optimization problem in (16) is feasible. Then, for $\Gamma_{req_k} > 0$ and $\Gamma_{tol} > 0$, a rank-one solution for the beamforming matrix, \mathbf{W}_k , of the SDP relaxed optimization problem in (16) can always be constructed, i.e., $\text{Rank}(\mathbf{W}_k) = 1, \forall k$.*

Proof: Please refer to the Appendix. ■

Theorem 1 states that the globally optimal solution of (16) can be obtained by information beamforming for each IR, despite the HWIs at the transceivers. Moreover, it can be shown

⁶We note that it can be shown that for the optimum solution of (16), constraints $\tilde{C}5$ and C10-C12 hold with equality, which allows us to exploit (16) for solving (13). The proof is omitted due to page limitation.

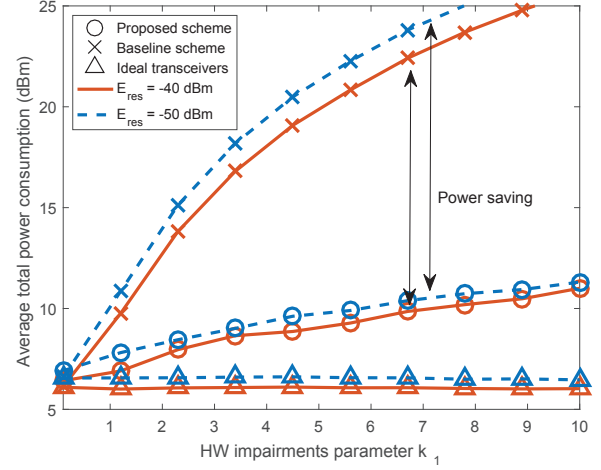


Fig. 2. Average total power consumption (dBm) versus HWI parameter k_1 for different amounts of residual energy E_{res} .

that energy beamforming is optimal for Phase I, even when the non-linearity of EH circuits and the residual HWIs are taken into consideration⁷. We note that we solve (16) for each $\tau_I \in [0, T_{\max}]$. Then, we obtain the globally optimum solution of (13) by employing a one-dimensional search over τ_I to find the minimum objective value.

V. NUMERICAL RESULTS

In this section, we evaluate the performance of the proposed resource allocation scheme for the considered WPCN. The relevant simulation parameters are provided in Table I. For conducting the one-dimensional search, we quantize the possible range of τ_I , $0 \leq \tau_I \leq T_{\max}$, into 20 equally spaced intervals, and for simplicity, we normalize the duration of the communication slot to $T_{\max} = 1$. The results obtained in this section were averaged over 1000 small scale fading realizations. Unless indicated otherwise, we assume for the transmitter HWI parameter $k_2 = 0.26$ and for the receiver HWI parameter $k_3 = 2$ [4]. The IRs are randomly distributed at a distance of 50 m around the AP. We assume that the data rate requirements of all IRs are equal, i.e., $R_{req_k} = R_{req} = 1$ bit/s, $\forall k$, while the maximum tolerable rate of Eve is $R_{tol} = 0.2$ bit/s. Besides, we assume $N_{PS} = 6$, $N_{AP} = 6$, and $N_{EV} = 3$ antennas at the PS, the AP, and Eve, respectively, unless specified otherwise.

In Figure 2, we show the total average power consumption versus the transmitter HWI parameter k_1 , cf. (5). The performance is illustrated for a WPCN with $K = 3$ IRs and for different values of residual energy E_{res} . As the HWI parameter k_1 increases, the total average power consumption of the proposed scheme also increases. This occurs because a higher value of k_1 reflects more severe transmit HWIs. As a result, because of the transmitter-side noise, the PS and the AP can focus their beams less accurately leading to an increased system power consumption. For comparison, we also consider the performance of a baseline scheme, which performs resource allocation subject to the same constraint set as in (13), but without taking the residual HWIs at the transceivers into consideration. The performance of the baseline scheme is then evaluated in the presence of the residual HWIs. As can be observed, the baseline scheme consumes significantly

⁷This can be proved by following a similar approach as in [14, Theorem 1]. The proof is omitted for brevity.

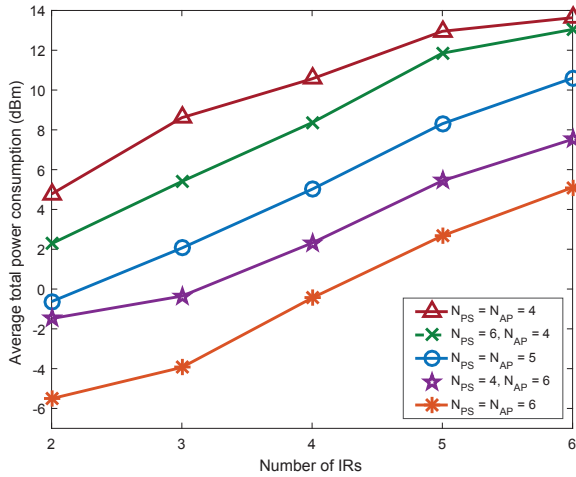


Fig. 3. Average total power consumption (dBm) versus number of IRs for different numbers of antennas at the PS, N_{PS} , and at the AP, N_{AP} .

more power compared to the proposed scheme. This is because of the model mismatch incurred by the baseline resource allocation scheme as the residual HWIs are ignored in the design phase. Moreover, in Figure 2, we have also included the performance for ideal transceivers. For ideal transceivers, the performance is independent of the HWI levels, of course, and serves as a performance upper bound for the proposed scheme. Figure 2 also shows that, as expected, a smaller amount of residual energy E_{res} at the AP increases the total average power consumption for all schemes as more power has to be transferred via WC.

In Figure 3, we depict the total average power consumption versus the number of IRs, K , for different numbers of antennas equipped at the PS, N_{PS} , and at the AP, N_{AP} . The residual energy is set to $E_{res} = -40$ dBm and the number of antennas at Eve is assumed to be $N_{EV} = 2$. Besides, the HWI model parameters are set to $k_1 = 2.3$, $k_2 = 0.26$, and $k_3 = 2$. As can be observed, having more IRs in the WPCN increases the total average power consumption substantially. This is because the QoS constraints on the minimum required data rate at each IR become more difficult to meet. Hence, more power is required for transmitting the desired information signals such that the QoS constraints are satisfied, which also increases the amount of power wasted due to the residual HWIs. On the other hand, the power consumption of the system is reduced when more antennas are equipped at the PS and the AP. With more antennas equipped at the PS and the AP, the degrees of freedom for resource allocation increase, which allows for a more accurate steering of the energy and information beams in the direction of the AP and the IRs, respectively. It can also be observed from Figure 3 that having more antennas at the AP is more beneficial than having more antennas at the PS for improving the average total power consumption of the proposed scheme. More antennas at the AP act as additional energy collectors and increase the amount of harvested power during Phase I. Hence, the power consumption of Phase I is reduced. Besides, when more antennas are equipped at the AP, there are extra degrees of freedom that can be exploited for a more precise information beamforming in the direction of the IRs, which results in a more efficient power allocation. Hence, having more antennas at the AP is beneficial for both transmission phases, whereas having more antennas at the PS is beneficial only for Phase I.

In Figure 4, we show the average duration of Phase I, τ_I ,

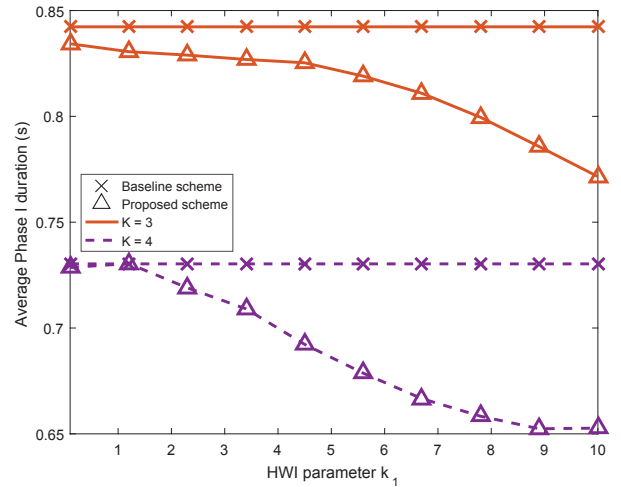


Fig. 4. Average Phase I duration τ_I versus HWI parameter k_1 for different number of IRs.

versus HWI parameter k_1 for $K = 3$ and $K = 4$ IRs. We assume $E_{res} = -40$ dBm and $N_{EV} = 3$. Besides, $k_2 = 0.26$, and $k_3 = 2$. As the HWI parameter k_1 increases, the optimal τ_I for the proposed scheme decreases⁸. The reason for this is that as the transmit HWIs become more severe, it becomes more difficult to meet the QoS constraints at each IR. Hence, a longer period for information transmission by the AP is needed, i.e., a larger τ_{II} , and the transmit power has to be increased, cf. Figure 2. Additionally, when there are more IRs in the WPCN, the optimal τ_I is smaller, since the required time for information transmission to meet the QoS constraints at all users increases. On the other hand, the duration of Phase I stays constant for the baseline scheme, since this scheme ignores the HWIs.

VI. CONCLUSIONS

In this paper, we studied the power-efficient resource allocation algorithm design for providing communication secrecy in a WPCN, where we took into account a practical non-linear EH model and the residual HWIs at the transceivers. The resource allocation algorithm design was formulated as a non-convex optimization problem for the minimization of the total consumed power subject to QoS constraints at the IRs. The optimal solution of the design problem was obtained via a one-dimensional search and SDP relaxation. Numerical results demonstrated the detrimental effects of residual HWIs on the performance of the WPCN. Moreover, the proposed scheme was shown to outperform a baseline scheme, which was designed under the assumption of ideal transceivers.

APPENDIX - PROOF OF THEOREM 1

The SDP relaxed problem in (16) satisfies Slater's constraint qualification and is jointly convex with respect to the optimization variables. Thus, strong duality holds and we can exploit the dual problem in order to study the structure of the solution. To this end, we consider an equivalent version of problem (16),

⁸We note that the τ_I for the proposed scheme and the baseline scheme are not necessarily identical for small values of k_1 as there are also HWIs at the receivers, i.e., $k_3 \neq 0$.

given by:

$$\begin{aligned}
& \underset{\mathcal{P}, \mathbf{A}_{\text{PS}}, \mathbf{A}_{\text{AP}}, \mathbf{A}_{\text{IR}}}{\text{minimize}} \quad \tau_{\text{I}} \widetilde{P}_{\text{PS-I}} + \tau_{\text{II}} \widetilde{P}_{\text{AP-II}} \quad (17) \\
& \text{s.t.} \quad \widetilde{\text{C1}}, \widetilde{\text{C2}}, \widetilde{\text{C4}}, \widetilde{\text{C5}}, \text{C6}, \text{C9}, \\
& \quad \widetilde{\text{C10}}: \eta_n \left(\sqrt{[\mathbf{A}_{\text{AP}}]_{n,n}} \right) \leq \sqrt{[\mathbf{B}_{\text{AP}}]_{n,n}}, \forall n \\
& \quad \widetilde{\text{C10a}}: [\mathbf{A}_{\text{AP}}]_{n,n} = \mathbf{S}_n \left(\sum_{k=1}^K \mathbf{W}_k + \mathbf{U} \right), \forall n, \\
& \quad \widetilde{\text{C11}}: \eta_m \left(\sqrt{[\mathbf{A}_{\text{PS}}]_{m,m}} \right) \leq \sqrt{[\mathbf{B}_{\text{PS}}]_{m,m}}, \forall m \\
& \quad \widetilde{\text{C11a}}: [\mathbf{A}_{\text{PS}}]_{m,m} = \mathbf{S}_m \mathbf{V}, \forall m \\
& \quad \widetilde{\text{C12}}: \nu \left(\sqrt{[\mathbf{A}_{\text{IR},k}]_{k,k}} \right) \leq r_{\text{IR},k}, \forall k. \\
& \quad \widetilde{\text{C12a}}: \mathbf{A}_{\text{IR},k} = \text{Tr} \left(\mathbf{H}_k \left(\sum_{t=1}^K \mathbf{W}_t + \mathbf{U} \right) \right), \forall k.
\end{aligned}$$

Then, we write the Lagrangian function of the SDP relaxed problem in (17):

$$\begin{aligned}
\mathcal{L} = & \rho_{\text{AP}} \tau_{\text{II}} (1 + \gamma) \left(\sum_{k=1}^K \text{Tr}(\mathbf{W}_k) + \text{Tr}(\mathbf{U}) \right) \\
& + \sum_{k=1}^K \alpha_k \left(-\frac{\text{Tr}(\mathbf{H}_k \mathbf{W}_k)}{\Gamma_{\text{req}_k}} + \text{Tr}(\mathbf{H}_k \sum_{j \neq k} \mathbf{W}_j) + \text{Tr}(\mathbf{U} \mathbf{H}_k) \right) \\
& + \sum_{k=1}^K \text{Tr} \left(\left(\mathbf{G}^H \left(\frac{\mathbf{W}_k}{\Gamma_{\text{tol}}} - \mathbf{U} \right) \mathbf{G} \right) \mathbf{D}_k \right) - \text{Tr}(\mathbf{U} \mathbf{Z}) \\
& - \sum_{n=1}^{N_{\text{AP}}} \mu_n \left(\mathbf{S}_n \left(\sum_{k=1}^K \mathbf{W}_k + \mathbf{U} \right) \right) - \sum_{k=1}^K \text{Tr}(\mathbf{W}_k \mathbf{Y}_k) \\
& - \sum_{k=1}^K \varrho_k \text{Tr}(\mathbf{H}_k (\sum_{k=1}^K \mathbf{W}_k + \mathbf{U})) + \Delta, \quad (18)
\end{aligned}$$

where $\alpha_k \geq 0, \gamma \geq 0, \mu_n \geq 0$, and $\varrho_k \geq 0$ are the dual variables associated with constraints $\widetilde{\text{C1}}, \widetilde{\text{C4}}, \widetilde{\text{C10a}}$, and $\widetilde{\text{C12a}}$, respectively. Moreover, $\mathbf{D}_k \succeq \mathbf{0}$ and $\mathbf{Y}_k \succeq \mathbf{0}, \mathbf{Z} \succeq \mathbf{0}$ are the Lagrangian multiplier matrices corresponding to constraints $\widetilde{\text{C2}}$ and C6 , respectively. Δ denotes the collection of terms not relevant for the proof. The Karush-Kuhn-Tucker (KKT) conditions needed for the proof are given by⁹:

$$\mathbf{D}_k^* \succeq \mathbf{0}, \mathbf{Y}_k^* \succeq \mathbf{0}, \forall k, \mathbf{Z}^* \succeq \mathbf{0} \quad (19)$$

$$\alpha_k^*, \varrho_k^* \geq 0, \forall k, \mu_n^* \geq 0, \forall n, \gamma^* \geq 0, \quad (20)$$

$$\mathbf{Y}_k^* \mathbf{W}_k^* = \mathbf{0}, \forall k, \mathbf{Z}^* \mathbf{U}^* = \mathbf{0}, \quad (21)$$

$$\nabla_{\mathbf{W}_k^*} \mathcal{L} = \mathbf{0}, \forall k, \nabla_{\mathbf{U}^*} \mathcal{L} = \mathbf{0}. \quad (22)$$

Combining both KKT conditions from (22), after some mathematical manipulations we can obtain:

$$\begin{aligned}
& \mathbf{Y}_k^* + \alpha_k^* \left(1 + \frac{1}{\Gamma_{\text{req}}} \right) \mathbf{H}_k \\
& = \underbrace{\mathbf{Z}^* + \sum_{j \neq k} \alpha_j^* \mathbf{H}_j + \mathbf{G} \mathbf{D}_k^* \mathbf{G}^H \left(1 + \frac{1}{\Gamma_{\text{tol}}} \right)}_{\mathbf{A}_k^* \succ \mathbf{0}}. \quad (23)
\end{aligned}$$

It can be shown that at the optimum solution of problem (17), constraint $\widetilde{\text{C1}}$ is satisfied with equality. Hence, $\alpha_k^* > 0, \forall k$ holds. Besides, matrix \mathbf{A}_k^* defined in (23) is a full rank matrix,

$\forall k$. It can be shown that if \mathbf{A}_k^* was not a full rank positive definite matrix, the dual optimum solution would become unbounded from below. Yet, the optimal value for the original primal problem is non-negative, due to $\Gamma_{\text{req}_k} > 0, \forall k, \Gamma_{\text{tol}} > 0$. Hence, we consider the case when $\text{Rank}(\mathbf{A}_k^*) = N_{\text{AP}}, \forall k$. By applying basic matrix rank algebra to (23), i.e., $\text{Rank}(\mathbf{A}) + \text{Rank}(\mathbf{B}) \geq \text{Rank}(\mathbf{A} + \mathbf{B})$, we obtain the following relation:

$$\begin{aligned}
& \text{Rank}(\mathbf{Y}_k^*) + \text{Rank} \left(\alpha_k^* \left(1 + \frac{1}{\Gamma_{\text{req}_k}} \right) \mathbf{H}_k \right) \\
& \geq \text{Rank} \left(\mathbf{Y}_k^* + \alpha_k^* \left(1 + \frac{1}{\Gamma_{\text{req}_k}} \right) \mathbf{H}_k \right) \\
& = \text{Rank}(\mathbf{A}_k^*) = N_{\text{AP}} \\
& \Rightarrow \text{Rank}(\mathbf{Y}_k^*) \geq N_{\text{AP}} - 1. \quad (24)
\end{aligned}$$

Hence, $\text{Rank}(\mathbf{Y}_k^*)$ can be either $N_{\text{AP}} - 1$ or N_{AP} . Since at the optimum solution, $\mathbf{W}_k^* \neq \mathbf{0}$, due to $\Gamma_{\text{req}_k} > 0, \forall k$, it follows from (21) that $\text{Rank}(\mathbf{Y}_k^*) = N_{\text{AP}} - 1$ and $\text{Rank}(\mathbf{W}_k^*) = 1, \forall k$. Hence, a rank-one solution for (16) is obtained. ■

REFERENCES

- [1] S. Bi, Y. Zeng, and R. Zhang, "Wireless Powered Communication Networks: An Overview," *IEEE Wireless Commun.*, vol. 23, no. 2, pp. 10–18, Apr. 2016.
- [2] M. Zorzi, A. Gluhak, S. Lange, and A. Bassi, "From Today's INTRANet to a Future INTERNet of Things: A Wireless- and Mobility-Related View," *IEEE Wireless Commun.*, vol. 17, no. 6, pp. 44–51, Dec. 2010.
- [3] Y. Wu, X. Chen, C. Yuen, and C. Zhong, "Robust Resource Allocation for Secrecy Wireless Powered Communication Networks," *IEEE Commun. Lett.*, vol. 20, no. 12, pp. 2430–2433, Dec. 2016.
- [4] E. Björnson, P. Zetterberg, and M. Bengtsson, "Optimal Coordinated Beamforming in the Multicell Downlink with Transceiver Impairments," in *Proc. IEEE Global Telecommun. Conf.*, Dec. 2012, pp. 4775–4780.
- [5] C. Studer, M. Wenk, and A. Burg, "MIMO Transmission with Residual Transmit-RF Impairments," *International ITG Workshop on Smart Antennas (WSA)*, pp. 189–196, Feb. 2010.
- [6] Y. Sun, D. W. K. Ng, J. Zhu, and R. Schober, "Multi-Objective Optimization for Robust Power Efficient and Secure Full-Duplex Wireless Communication Systems," *IEEE Trans. Wireless Commun.*, vol. 15, no. 8, pp. 5511–5526, Aug. 2016.
- [7] D. Ng and R. Schober, "Secure and Green SWIPT in Distributed Antenna Networks With Limited Backhaul Capacity," *IEEE Trans. Wireless Commun.*, vol. 14, pp. 5082–5097, Sep. 2015.
- [8] X. Chen, J. Chen, and T. Liu, "Secure Transmission in Wireless Powered Massive MIMO Relaying Systems: Performance Analysis and Optimization," *IEEE Trans. Veh. Technol.*, vol. 65, no. 10, pp. 8025–8035, Oct. 2016.
- [9] X. Chen, D. W. K. Ng, and H. H. Chen, "Secrecy Wireless Information and Power Transfer: Challenges and Opportunities," *IEEE Wireless Communications*, vol. 23, no. 2, pp. 54–61, Apr. 2016.
- [10] J. Zhu, D. W. K. Ng, N. Wang, R. Schober, and V. Bhargava, "Analysis and Design of Secure Massive MIMO Systems in the Presence of Hardware Impairments," *IEEE Trans. Wireless Commun.*, pp. 2001–2016, Jan. 2017.
- [11] W. Liu, X. Zhou, S. Durrani, and P. Popovski, "Secure Communication With a Wireless-Powered Friendly Jammer," *IEEE Trans. Wireless Commun.*, vol. 15, no. 1, pp. 401–415, Jan. 2016.
- [12] D. K. Nguyen, M. Matthaiou, T. Q. Duong, and H. Ochi, "RF Energy Harvesting Two-way Cognitive DF Relaying with Transceiver Impairments," in *Proc. IEEE Intern. Commun. Conf.*, Jun. 2015, pp. 1970–1975.
- [13] J. Guo and X. Zhu, "An Improved Analytical Model for RF-DC Conversion Efficiency in Microwave Rectifiers," in *IEEE MTT-S Int. Microw. Symp. Dig.*, Jun. 2012, pp. 1–3.
- [14] E. Boshkovska, D. W. K. Ng, N. Zlatanov, A. Koelpin, and R. Schober, "Robust Resource Allocation for MIMO Wireless Powered Communication Networks with Non-linear EH Model," *IEEE Trans. Commun.*, vol. PP, no. 99, pp. 1–1, Feb. 2017.
- [15] T. Schenk, *RF Imperfections in High-Rate Wireless Systems: Impact and Digital Compensation*. Springer Publishing, 2010.
- [16] E. Boshkovska, D. Ng, N. Zlatanov, and R. Schober, "Practical Non-linear Energy Harvesting Model and Resource Allocation for SWIPT Systems," *IEEE Commun. Lett.*, vol. 19, no. 12, pp. 2082–2085, Dec. 2015.
- [17] M. Grant and S., "CVX: Matlab Software for Disciplined Convex Programming, version 2.0 beta," [Online] <https://cvxr.com/cvx>, Sep. 2012.

⁹We denote the optimal solution for optimization variable x by x^* .